Immunity, Vol. 19, 595–606, October, 2003, Copyright ©2003 by Cell Press

A Correlation between TCR Vα Docking on MHC and CD8 Dependence: Implications for T Cell Selection

Jennifer Buslepp,[1] Huanchen Wang,[1] William E. Biddison,[5] Ettore Appella,[4] and Edward J. Collins[1,2,3,*]

[1]Department of Biochemistry and Biophysics
[2]Department of Microbiology and Immunology
[3]Lineberger Comprehensive Cancer Center
University of North Carolina
Chapel Hill, North Carolina 27599
[4]Laboratory of Cell Biology
National Cancer Institute
National Institutes of Health
Bethesda, Maryland 20892
[5]Molecular Immunology Section
Neuroimmunology Branch
National Institute of Neurological Disorders and Stroke
National Institutes of Health
Bethesda, Maryland 20892

Summary

T cell receptors (TCR) adopt a similar orientation when binding with major histocompatibility complex (MHC) molecules, yet the biological mechanism that generates this similar TCR orientation remains obscure. We show here the cocrystallographic structure of a mouse TCR bound to a human MHC molecule not seen by the TCR during thymic development. The orientation of this xenoreactive murine TCR atop human MHC deviates from the typical orientation more than any previously determined TCR/MHC structure. This unique orientation is solely due to the placement of the TCR Vα domain on the MHC. In light of new information provided by this structure, we have reanalyzed the existing TCR/MHC cocrystal structures and discovered unique features of TCR Vα domain position on class I MHC that correlate with CD8 dependence. Finally, we propose that the orientation seen in TCR recognition of MHC is a consequence of selection during T cell development.

Introduction

Clonotypic αβ T cell receptors (TCR) on the T cell surface specifically interact with peptides bound to major histocompatibility complex (pMHC) molecules. Recognition of the pMHC by the TCR is required for activation and subsequent killing by cytolytic T cells. Proper immune system function requires a large repertoire of T cells that are responsible for recognition of any foreign peptide bound to self-MHC. This large repertoire of T cells is created by splicing of TCR variable domains containing complementarity determining regions CDR1 and CDR2, and by joining of TCR variable and constant domains to form the CDR3 region in both the α and β chains (reviewed in Davis and Bjorkman, 1988). The polymorphic CDR regions make all the contacts with the MHC and peptide, with the CDR3 loops positioned over the center of the peptide in the peptide binding groove of the MHC (Garboczi and Biddison, 1999; Garboczi et al., 1996). Thus, the most variable region of the TCR is centered on the most variable region of the pMHC.

The cocrystal structures of TCR and pMHC determined to date have shown a similar docking orientation of TCR on pMHC. The TCR Vα domain is positioned over α2 of the MHC near the amino terminus of the peptide, while the Vβ domain is found atop the MHC α1 domain near the carboxyl terminus of the peptide (Garboczi and Biddison, 1999; Rudolph and Wilson, 2002). The KB5-C20 TCR was recently shown to undergo large conformational change upon binding of pKB1/K^b in order to preserve this binding mode (Reiser et al., 2002). The TCR/MHC binding angle is often referred to as "diagonal," yet the existing crystallographic data demonstrates that the angle the TCR makes with the peptide binding groove of the MHC may vary from ~45° to 80° (Rudolph and Wilson, 2002). The most recent spectacular departure from a diagonal orientation comes from an immunodominant flu-specific, A2-restricted TCR JM22 (Stewart-Jones et al., 2003). When the first class II MHC/TCR structure was determined, it was speculated that Class II-restricted TCR bound in an orthogonal manner while Class I-restricted TCR conformed to a diagonal orientation (Reinherz et al., 1999). However, this idea of orthogonally oriented Class II-restricted TCR and diagonally oriented Class I TCR was proposed when few Class I MHC/TCR structures were available. Currently, the existing TCR/pMHC structural database puts the orientation angle for Class II-restricted TCR into the range of angles seen for Class I-restricted TCR.

It would be reasonable to expect that the common mode of binding would be governed by a set of conserved interactions between the TCR and pMHC. Surprisingly, no conserved interactions have been identified in the different cocrystal structures of MHC and TCR that explain the common docking. Additionally, alanine scanning mutagenesis of both TCR and pMHC contact surfaces have failed to identify residues that are crucial for determining that orientation (Baker et al., 2001; Manning et al., 1998; Wang et al., 2002).

During T cell development in the thymus, T cells are selected based on their ability to recognize self-MHC molecules. Although the molecular mechanisms underlying T cell selection are not entirely clear, mounting experimental evidence supports a quantitative/avidity model of thymocyte selection, which predicts that avidity of the TCR/MHC interaction determines whether or not an immature T cell will survive the selection process (Sebzda et al., 1999). Thus, during positive selection, those thymocytes that survive will have at least low avidity for self-pMHC. Conversely, presumably in order to avoid rampant autoimmune disease, high avidity T cells are eliminated by apoptosis during negative selection.

In addition to the processes of positive and negative

*Correspondence: edward_collins@med.unc.edu

selection, immature thymocytes make a CD4 or CD8 lineage commitment while in the thymus. Instructional and stochastic models of lineage commitment have been proposed. The instructional model says that commitment is controlled with a unique signal specifying differentiation into $CD4^+$ or $CD8^+$ T cells. The stochastic model says the decision to become $CD4^+$ or $CD8^+$ T cells is random, and T cells that make the wrong decision are eliminated. Recent data support the instructional model. The popular "strength of signal" theory proposes that short duration $p56^{lck}$ signals result in CD8 commitment, while higher intensity/longer duration signals result in CD4 commitment (Germain, 2002). Regardless of the exact mechanism, the outcome of T cell development is a finely tuned repertoire of $CD4^+$ and $CD8^+$ T cells, responsible for the identification of all foreign antigens, but only in the context of self-MHC.

Although detection of foreign peptides bound to self-MHC is the function of T cells, it is estimated that 1%–10% of TCR react to non-self MHC molecules (alloreactivity or xenoreactivity). The ability of a single TCR to recognize two distinct peptide/MHC complexes, termed T cell crossreactivity, occurs frequently and has been suggested to be critical to recognition of foreign antigen (Mason, 1998). It had been proposed that T cell crossreactivity was the result of similarities in the charge and/or shape of the antigenic surface presented to the TCR, an idea termed molecular mimicry. Recent structural studies of crossreactive TCR ligands demonstrate that crossreactivity is not necessarily due to any obvious resemblance between pMHC surfaces (Reiser et al., 2003; Zhao et al., 1999). Instead, studies with altered peptide ligands (APL) and the cocrystal structures of TCR bound to pMHC ligands have highlighted the plasticity of TCR antigen recognition (Ding et al., 1999; Garcia et al., 1998). In fact, when TCRs with high affinity and high peptide specificity (hence presumably less plasticity) were made in vitro, crossreactivity increased dramatically (Holler et al., 2003).

It is not known whether TCR that recognize a MHC from a different species would interact in a different manner than found for TCR recognition of self-MHC. Xenoreactivity is of particular interest, as no evolutionary advantage would be conferred to a species' T cells that retain the ability to recognize MHC from another species, since divergence occurred several million years ago. Nevertheless, xenografts are eventually rejected due, in part, to the T cell cytotoxicity resulting from MHC mismatch. In order to examine this phenomenon in detail, we are studying a murine-derived AHIII 12.2 T cell as a model for xenogeneic transplant rejection. AHIII 12.2 T cells were selected in the $H2^b$ mouse (C57Bl/6), but are xenoreactive (Engelhard and Benjamin, 1982) and recognize the human MHC HLA-A*0201 (A2) and a human self-peptide called p1049 (Henderson et al., 1993). The AHIII 12.2 T cell also recognizes mouse class I MHC, H2-D^b (D^b) and the peptide (p1058) (Loftus et al., 1997). The AHIII 12.2 T cell is CD8 independent with respect to recognition of the human pMHC (p1049/A2), yet proliferation and cytolysis are not different from engagement of a pMHC ($p1058/D^b$) that requires CD8 (Buslepp et al., 2003). The crystal structures of p1049/A2 and $p1027/D^b$ show that AHIII 12.2 TCR cannot recognize similar molecular surfaces (Zhao et al., 1999).

In order to examine xenoreactive TCR/pMHC interactions directly, the ectodomains from the α and β chains of the AHIII 12.2 TCR were cloned from the AHIII 12.2 T cell and expressed in *E. coli* (Buslepp et al., 2003). The cocrystallographic structure of the murine AHIII 12.2 TCR bound to human HLA-A2 with the peptide p1049 (ALWGFFPVL) was determined. This xenoreactive murine TCR docks almost exactly perpendicular to the peptide binding groove of the human pMHC, and thus is the furthest departure from a "diagonal" orientation seen so far for a TCR/pMHC cocrystal complex. This deviation from the current structural ideology of TCR and pMHC when examined with other biological data suggests a requirement for a specific molecular geometry during T cell selection.

Results

Crystallographic data (30–2.0 Å) were collected from a single crystal of the ectodomains of the murine TCR AHIII 12.2 and the human class I MHC complex p1049/A2 (ALWGFFPVL). The unambiguous molecular replacement solution showed two identical complexes of TCR/pMHC in the asymmetric unit. The crystallographic structure is well refined to an R_{free} of 25.3% from 30.0–2.0 Å. Data and refinement statistics may be found in Table 1. The structure of p1049/A2 has no significant differences when compared to the uncomplexed protein (Zhao et al., 1999). The structure of the AHIII TCR is similar to the structures of other TCR determined to date (Ding et al., 1998; Garboczi et al., 1996; Garcia et al., 1998; Hennecke et al., 2000; Kjer-Nielsen et al., 2003; Reinherz et al., 1999; Reiser et al., 2000, 2002; Stewart-Jones et al., 2003). The TCR of the xenoreactive complex is bound to the MHC peptide binding cleft in a manner analogous to recognition of other TCR examined crystallographically (Figure 1). The variable domains are positioned above the peptide binding groove with the CDR3 loops from each chain positioned above the center of the peptide. The positions of the constant domains relative to the variable domains of the AHIII 12.2 TCR are slightly different from other individual TCR (not shown), but these changes are within the range found in the structures of TCRs in general (Rudolph and Wilson, 2002).

There are two nearly identical copies of the TCR/pMHC complexes in the asymmetric unit of the crystal. These TCR/pMHC complexes are in the same orientation such that a simple lateral translation relates the two copies. These two complexes suggest a manner for TCR oligomerization on T cells that has been previously proposed to be important for T cell signaling (Bachmann et al., 1998; Rotzschke et al., 1997). However, when the structure of A2 bound to CD8 is superimposed on one copy of p1049/A2 bound to AHIII 12.2 (Gao et al., 1997; Kern et al., 1998), the CD8 molecule and the TCR from the second p1049/A2/AHIII 12.2 complex occupy the same location in space. Therefore, we conclude that this pair of complexes cannot represent a physiologically meaningful oligomer, and that this dimer is a crystallization artifact.

Table 1. Data and Refinement Statistics for AHIII 12.2:p1049/A2

Data Collection	
Space Group	$P2_1$
Cell Dimensions	a = 93.71 Å, b = 84.47 Å, c = 121.34 Å, β = 92.13°
Molecules/AU	2
Resolution	30.0–2.0 Å
R_{merge}(%)[a]	7.4 (57.8)
$<I/\sigma>$	28.5 (3.5)
Unique reflections	121,366
Average redundancy	7.5
Completeness (%)	99.9 (99.9)
Solvent content	46%
Refinement	
Resolution Range	30.0–2.0 Å
Number Reflections (Rfac/Rfree)	114,945/6,421
R_{fac}	21.9 (24.4)
R_{free}	25.3 (29.4)
Number of non-hydrogen atoms	13,255
Number water molecules	432
Mean B value	14.2 Å^2
Coordinate error	0.179 Å
<Rs fit>	89.0%
Deviations from ideality	
—Bond lengths	0.012 Å
—Bond angles	1.435°
Ramachandran	
Most favorable	89.7%
Additionally allowed	9.9%
Generously allowed	0.4%
Disallowed	0.0%

[a] $R_{merge} = \Sigma_{hkl} \Sigma_i |I_i - <I>| / \Sigma_{hkl} \Sigma_i I_i$, where I_i is the observed intensity and $<I>$ is the average intensity of multiple observations of symmetry related reflections.

[b] Number in parenthesis refers to the highest resolution shell (2.05–2.00 Å)

[c] $R = \Sigma_{hkl} ||F_{obs}| - k|F_{cal}|| / \Sigma_{hkl} |F_{obs}|$, where R_{free} is calculated for a randomly chosen 5% of reflections, R_{work} is calculated for the remaining 95% of reflections used for structure refinement. Numbers in parenthesis refer to the number of structure factors used in the measurements.

[d] <Rs fit> is the average real space fit of all atoms on a 2fo-fc electron density map.

[e] Error is the mean coordinate error estimate based on maximum likelihood measurements (Murshudov, 1997; Pannu and Reed, 1996)

Orientation of TCR Docking on pMHC

Structural studies of four human Class I pMHC complexes with unique human TCR (TCR = A6, B7, and LC13 and JM22) and three mouse Class I pMHC complexes with unique murine TCR (TCR = 2C, BM3.3, and KB5-C20) have established that TCR dock diagonally with respect to the orientation of the peptide in the peptide binding groove with large variances in the diagonal nature (reviewed in Rudolph and Wilson, 2002). Figures 2A–2G show the molecular surface of the variable domains of the TCR atop the pMHC surface shown in shades of gray. The molecular surfaces of these previously published TCR are shown in various colors, to compare the orientation with respect to the molecular surface of the AHIII 12.2 TCR shown in green in each panel. These data show that orientation of AHIII 12.2 is significantly different from the other TCRs (except JM22) and is not in a diagonal orientation when bound to p1049/A2. Figure 2H shows the orientations of the TCR schematically with a ball representing the center of mass of each variable domain. The angle that these TCR take with respect to the path of the peptide spans from 44° to 84° for TCR other than AHIII 12.2; AHIII 12.2 docks at 89°. It is clear from the comparison that the orientation of the variable domains are not fixed at a specific position on the MHC particularly with respect to the lateral position of the domain along the peptide. 2C, KB5-C20, A6, and B7 are found in a common orientation. The entire BM3.3 and LC13 TCRs are found shifted toward the carboxyl terminal end of the peptide. The orientation of the AHIII 12.2 TCR may be described as orthogonal to the direction of the peptide. This is similar to the recently described structure of the immunodominant TCR JM22 (Stewart-Jones et al., 2003), but more pronounced in terms of the orthogonality. Additionally, the Class II-restricted TCR D10 and HA1.7 have been termed orthogonal (Hennecke et al., 2000; Reinherz et al., 1999), but at 80° and 70°, respectively, these two TCRs bind MHC in a more diagonal orientation than AHIII 12.2 and JM22 (Figure 2I; Table 2). The large distribution of TCR positions suggests that the angle (orientation) of binding of TCR to pMHC is not critical to T cell function.

The center of mass of the Vα domain of AHIII 12.2 is found almost midway between the amino and carboxyl termini of the peptide (Figure 2H). Interestingly, the positions of the Vα domains' of the Class I-restricted TCR seem to cluster into two distinct sets. Four Vα domains cluster together at a position closer to the amino terminus of the peptide. Group a includes 2C, A6, B7, and KB5-C20. Group b includes BM3.3, LC13, JM22, and AHIII 12.2 with Vα domains significantly different from those of the group a position. As compared to the average position of all eight domains, the two groups are significantly different using a grouped-pair Student's T test ($p = 0.01$). When compared to the average position of group b (represented by BM3.3, LC13, AHIII12.2, and JM22 in Figure 2h), the positions of each of the other four are significantly different ($p < .003$). The Vβ domains also appear to group into two locations, one near the center and the other toward the carboxyl terminus of the peptide. Attempts to rationalize these groupings suggested some functional importance to the position of the Vα or Vβ domain and that BM3.3, LC13, JM22, and AHIII 12.2 share a common but as yet unknown feature. What was found is BM3.3 (Guimezanes et al., 2001), LC13 (S. Burrows and B. Jakobsen, personal communication), JM22 (Lawson et al., 2001), and AHIII 12.2 (Buslepp et al., 2003) are all CD8 independent. These data are summarized in Table 2.

Interactions between AHIII 12.2 and p1049/A2

AHIII 12.2 xenoreactively recognizes p1049/A2. We suspected that the interactions between murine AHIII 12.2 TCR and human p1049/A2 may be different than observed from other TCR/pMHC complexes because the mouse AHIII 12.2 did not encounter HLA-A2 during T cell selection. Some differences are observed during xenoreactive T cell recognition, as opposed to syn or allorecognition. There are significantly more interactions (H bonds, water bridges, van der Waals interactions between 2 and 4 Å) between AHIII 12.2 and p1049/A2 (163) than seen for other TCR/pMHC complexes ($p = 0.003$). The next closest TCR with a large number of interactions is LC13 with 150 followed by A6 with 127 interactions.

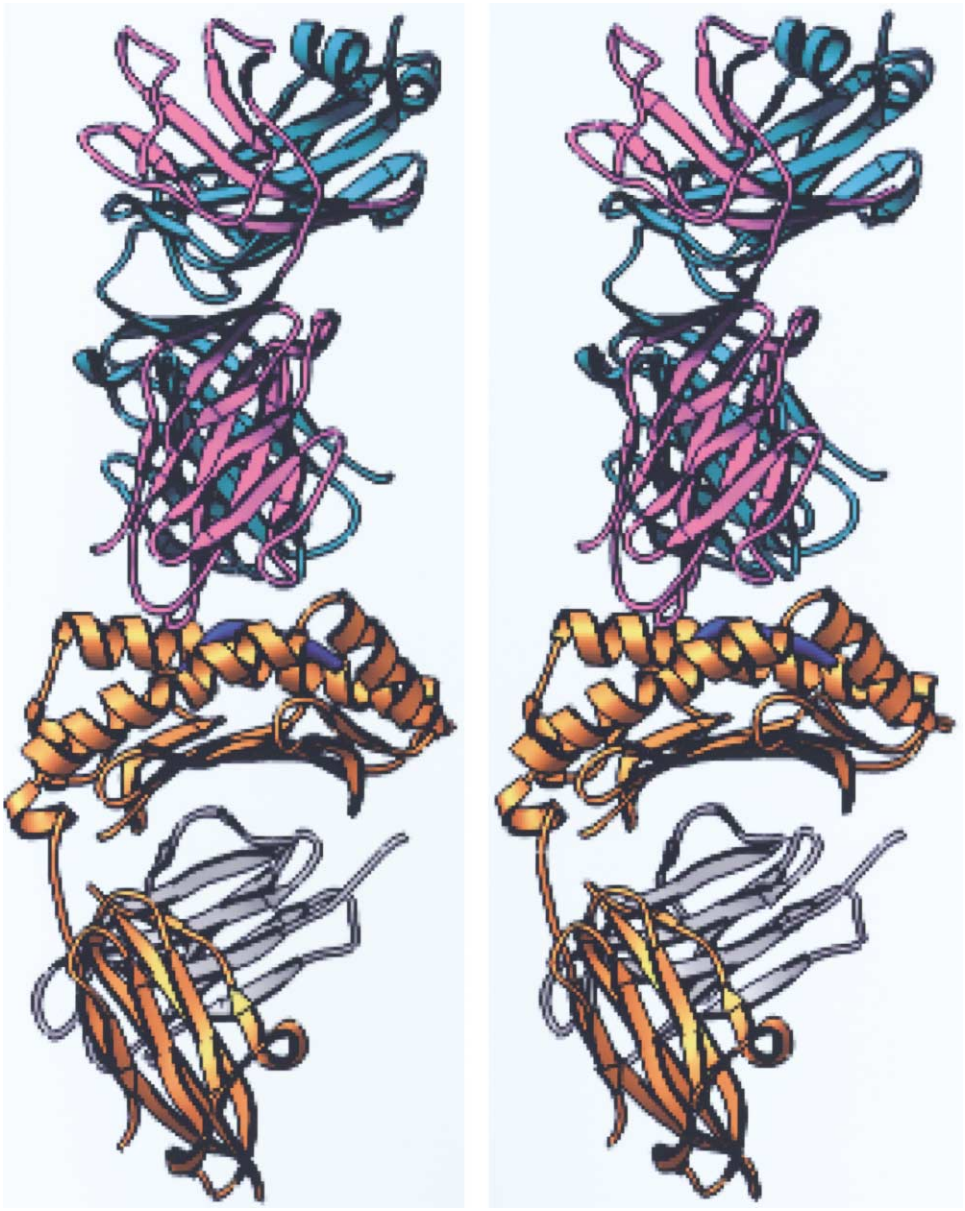

Figure 1. The Structure of AHIII 12.2 Bound to Xenogeneic p1049/A2

The stereo view of AHIII 12.2 TCR is depicted as a ribbon (Carson, 1987) in magenta (α chain) and blue (β chain). The A2 heavy chain is silver, β_2m is cyan, and the p1049 peptide is gold.

The largest differences in interactions are found between the AHIII 12.2 Vα domains and Vα domains of other pMHCs (Figure 3A). In AHIII 12.2 and p1049/A2, the pMHC/Vα interactions are dominated by van der Waals contacts to the MHC. The other TCR have more equally distributed types of interactions, and interactions with the peptide predominate. It appears reasonable to suggest that large numbers of specific interactions between TCR and MHC would result in high self-affinity and negative selection. AHIII 12.2, which was not selected on A2 during development in the thymus, may use more van der Waals contacts to recognize p1049/A2, specifically because since it did not go through selection on A2, it was not negatively selected and survived. Alloreactive TCR appear to preferentially use their β chains to make the majority of interactions (Rudolph and Wilson, 2002), but the number and type of interactions found between the Vβ domain of AHIII 12.2 and p1049/A2 are not increased as compared to other TCR Vβ domains (Figure 3B).

The total surface of A2 buried by AHIII 12.2 TCR (981 Å^2) is very similar to the average buried surface area (957 Å^2 sd = 164 Å^2) of other complexes (Figure 3C). The buried surface area of the p1049 peptide (250 Å^2) is not significantly different from the mean of other peptides (226.7 Å^2, sd = 72 Å^2). Although the shape comple-

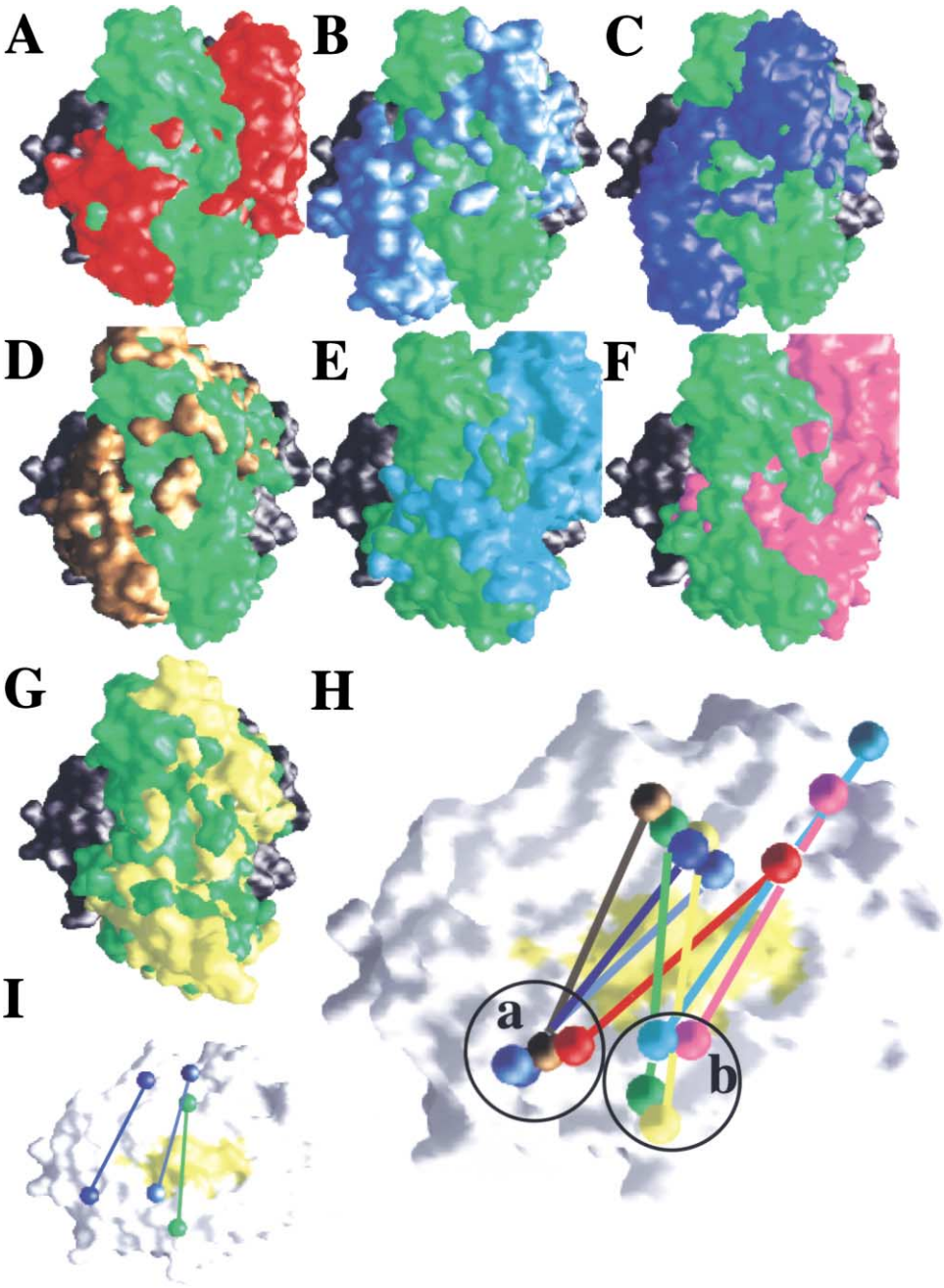

Figure 2. The Orientations of TCR Docked on Class I MHC Are Not Conserved to Diagonal

The orientation of AHIII 12.2 docking is most orthogonal when compared to other TCR/pMHC structures and Vα positions fall into two distinct groups. Class I MHC from TCR/pMHC cocrystal structures were superimposed onto p1049/A2 bound to AHIII 12.2. Molecular surfaces of the Vα and Vβ domains from those TCR are shown in addition to the variable domains of AHIII 12.2 (green) in order to compare the orientations of the TCR on the MHC. (A) 2C (red), (B) KB5-C20 (light blue), (C) A6 (dark blue), (D) B7 (gold), (E) BM3.3 (cyan), and (F) LC13 (magenta). (G) JM22 (yellow). (H) The positions of the center of mass of each TCR Vα and Vβ domain are given pseudo-atoms and the positions connected by a line to demonstrate the orientation that each TCR docks onto the MHC. The different TCR are colored as in (A)–(G). The p1049/A2 complex is shown as a molecular surface representation with the peptide colored yellow. (I) The orientation of Vα/Vβ pairs of TCR docking on class II MHC compared to AHIII 12.2. HA1.7 is shown in dark blue and D10 in light blue. AHIII 12.2 is shown in green. (A)–(I) were constructed with Grasp (Nicholls et al., 1991).

mentarity of the interface between AHIII 12.2 and p1049/A2 is the highest of the cocrystal structures examined to date at 71.6%, and approaches that of antibody:antigen interactions (Lawrence and Coleman, 1993), it is not significantly different from the complementarity seen in the other TCR/pMHC cocrystal structures (Figure 3D).

Table 2. Correlation of TCR Vα Position and CD8 Dependence

TCR/pMHC	Group by Vα position (Figure 2h)	CD8-dependent?	Docking Angle
AHIII 12.2/p1049/A2	a	No (Buslepp et al., 2003)	89°
BM3.3/pBM1/K^b	a	No (Guimezanes et al., 2001)	58°
LC13/FLRGRAYGL/B8	a	No (Sewell et al, 1999)	57°
JM22/MP/A2	a	No (Lawson et al., 2001)	84°
2C/SIYR/K^b	b	Yes (Daniels et al., 2000)	44°
A6/Tax/A2	b	Yes (data not shown)	58°
B7/Tax/A2	b	Yes (data not shown)	72°
KB5-C20/pKB1/K^b	b	Yes (Guimezanes et al. 2001)	45°

Docking angles are measured as the angle from the line formed by the amino and carboxyl ends of the class I MHC bound peptide.

The worst surface complementarity described is between the 2C TCR and SIYR/K^b (Garcia et al., 1998). However, surface complementarity also does not strictly correlate with affinity between the complexes. The affinity of AHIII 12.2 is relatively high (~10 μM) (Buslepp et al., 2003), but it is not higher than the affinities observed between other TCR/pMHC whose cocrystal structures have been determined (Rudolph and Wilson, 2002)

Recognition of Peptide

As observed in other TCRs cocrystallized with pMHC, the interactions of AHIII 12.2 with peptide are primarily

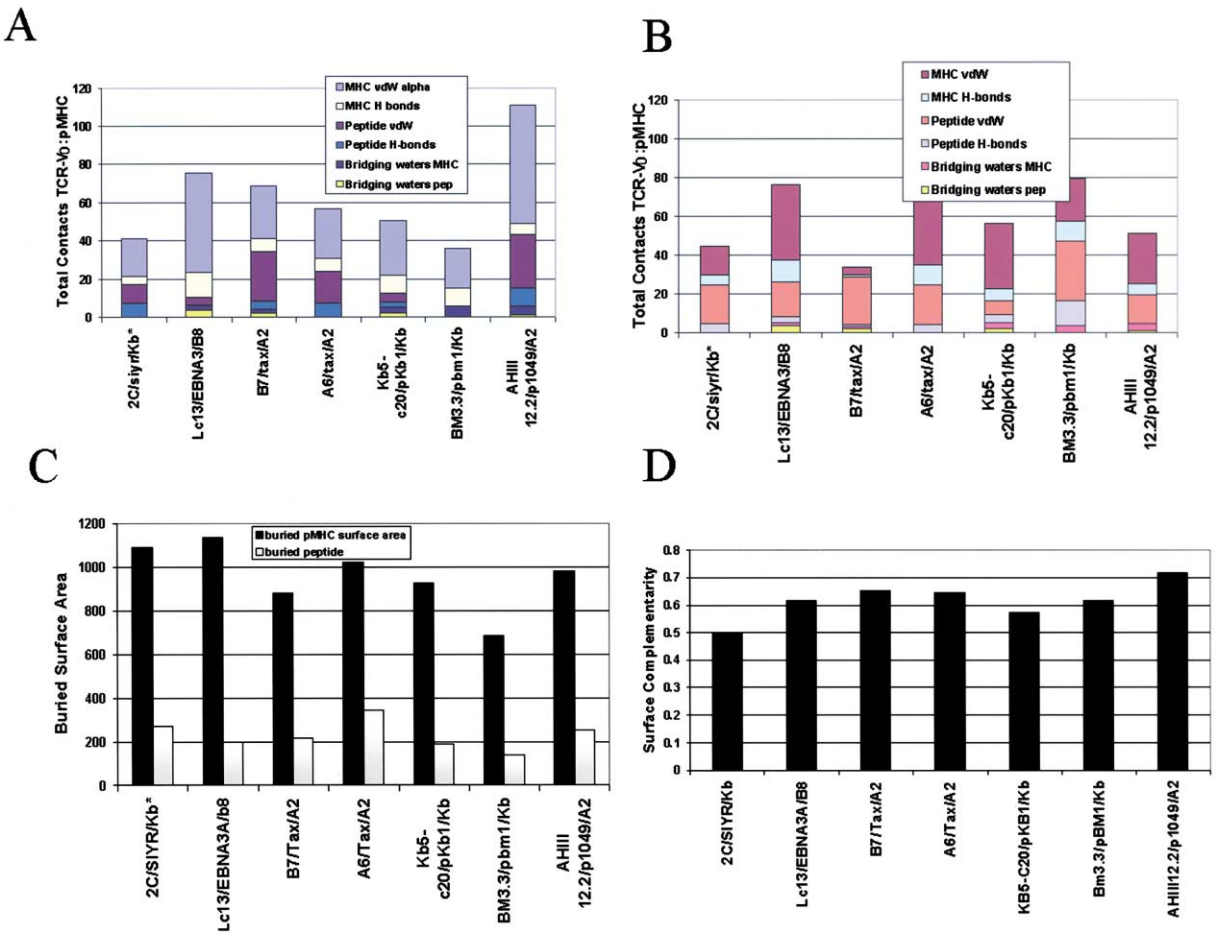

Figure 3. Comparison of the Interactions between AHIII 12.2 and p1049/A2 Other TCR/pMHC Complexes

(A) The contacts between TCR Vα domains and pMHC within 4.0 Å are divided into van der Waals (vdW) for MHC (or peptide) or hydrogen bonds (H-bonds) for MHC (or peptide) and for waters that make hydrogen bonds with both TCR and MHC or peptide (bridging) with color-coding as shown in the legend. Note that not all structures were of sufficient resolution to include waters in the model. Residues with 2.0 and 4.0 Å were determined using the program Contact (Dodson, 1997).

(B) The contacts between TCR Vβ domains with pMHC as shown as described in (A).

(C) Buried surface area of MHC or peptide for each peptide/Class I MHC/TCR complex (Dodson, 1997).

(D) Shape complementarity of each TCR for pMHC as calculated with sc (Lawrence and Coleman, 1993) and implemented in ccp4 (Dodson, 1997).

Table 3. Contacts between AHIII 12.2 TCR and p1049/A2

TCR	pMHC	TCR	pMHC
CDR1α		CDR1β	
Y28	G162	Y31	pF6
	T163		
	E166		
	W167		
S29	A158		
S31	E154		
	Q155		
	A158		
CDR2α		CDR2β	
TCR	pMHC	TCR	pMHC
F50	H151	Y48*	R65
	E154	Y50	K68
T51	H151	V51	Q72
		E56	R65
CDR3α		CDR3β	
TCR	pMHC	TCR	pMHC
E93	Q155	W97	K146
	pF5		W147
A97	pW3		A150
	pG4		V152
	pF5		pF5
S98	A158		pF6
	Y159		pP7
	T163		pV8
	pW3	V98	A150
	pG4	S99	pF5
S99	K66	Y100	A149
	T163		A150
F101	K65		Q155
	A69	F101	pF6
S102	pF5		

The "p" before a pMHC residue denotes that contact comes from the peptide p1049.3

mediated by the α and β chain CDR3 loops (Table 3). The p1049 central residues, P5 and P6, are phenylalanine, and both rings are oriented edge on to the TCR. In combination with the aliphatic residues on the A2 α helices, this produces a rather flat interaction surface that results in little interpenetration of either the peptide or the TCR side chains during binding. There are an equivalent number of contacts between the peptide and the variable domains of the α and β chains of the TCR, but the mechanism of interaction is different between the two domains. The CDR1α and CDR2α loops do not interact with peptide. CDR3α uses six residues to make seven contacts from the Trp at P3 to the Phe at P5. The CDR1β makes one contact with p1049/A2 with the Phe at P6. Like the CDR2α chain, CDR2β makes no contacts with the peptide. CDR3β uses five amino acids to make six contacts with the peptide.

Recognition of MHC

There are no conserved contacts between pMHC and TCR observed in the cocrystals of TCR/pMHC to date (Rudolph and Wilson, 2002). Instead, there are regions that are consistently involved in binding by virtue of the limited number of possibilities given the conserved docking orientation. However, the regions that the murine AHIII 12.2 TCR uses to interact with human p1049/A2 are different from the structures of the six of the seven previously examined Class I pMHC/TCR structures. The CDR1α loop of AHIII 12.2 interacts with residues 154,155,158, 162, 163, and 167 of p1049/A2; other TCR CDR1αs interact with residues around 58 and 62. The nearly orthogonal JM22 TCR uses many fewer CDR1α contacts, but those that it does make are at residues 154 and 155, like AHIII 12.2. The AHIII 12.2 CDR2α interacts with MHC residues around 151 as does JM22. However, in other TCRs, the CDR2α loops contact residues near 158 (not 151). The CDR3α of AHIII 12.2 interacts with MHC residues across the peptide binding groove. AHIII 12.2 interacts with 65 and 69 of the α1 domain of A2 and 155, 158, 159, and 163 of the α2 domain of A2. CDR3α of other TCR rarely interact with residues in the α2 domain (except for one contact in LC13 and one in KB5-C20). The CDR1β loop of AHIII 12.2 interacts with the peptide at phenylalanine at P6 but not the MHC; other TCRs interact with MHC residues around 76. The CDR2β loop of AHIII 12.2 interacts with residues around 68 (65, 68, and 72); the CDR2β loops of other TCRs interact with residues around 76, but not 68. The CDR3β chain contacts MHC residues solely in the α2 domain of A2 (146, 147, 149, 150, 152, and 155). Therefore, the types and quantities of interactions that AHIII 12.2 uses to recognize p1049/A2 may appear to be similar to recognition by other TCRs, but the specific MHC residues involved are different (Table 3).

Discussion

The murine T cell AHIII 12.2 recognizes human pMHC p1049/A2, and the crystal structure of this murine TCR in complex with its human pMHC ligand proves that xenoreactive recognition is functionally equivalent to recognition of pMHC by any TCR. Indeed, recognition by AHIII 12.2 has been shown to be peptide specific (Loftus et al., 1997), analogous to normal TCR recognition of syngeneic pMHC. However, the AHIII 12.2 TCR is bound to p1049/A2 in an orientation that is nearly perpendicular to the direction of the p1049 peptide, unlike the more diagonal TCR binding in previously characterized TCR/pMHC complexes. Binding of AHIII 12.2 TCR to p1049/A2 is tight (~10 μM) (Buslepp et al., 2003), but not tighter than the previously characterized TCR/pMHC structures. This clearly shows that a specific TCR orientation is not required for pMHC binding of sufficient affinity to activate normal CTL function (Buslepp et al., 2003). The number of contacts AHIII 12.2 makes with p1049 and HLA-A2 are not less than that of other TCR, demonstrating that a diagonal TCR orientation is not required for adequate interactions with peptide or MHC.

Although the TCR orientation adopted by AHIII 12.2 during recognition of p1049/A2 is atypical, it is unreasonable to assume that this anomaly is the result of a unique property of the AHIII 12.2 TCR. The AHIII 12.2 TCR also recognizes H2 D^b in complex with peptide p1058 in a syngeneic manner, and while a structure of AHIII 12.2 in complex with D^b-p1058 would undoubtedly add important information to our analysis, extensive efforts to crystallize the AHIII 12.2 with D^b-p1058 have been unsuccessful. Nonetheless, earlier peptide mutagenesis studies that compared the influence of alanine-

scanning mutations in p1049 (bound to A2) and p1058 (bound to D^b) on CTL lysis by AHIII 12.2 demonstrated that while mutations to the center of the p1049 peptide inhibited A2-mediated CTL activity, mutations at the C-terminal end of the p1058 peptide abrogated CTL lysis of p1058/D^b (Loftus et al., 1997). These results are consistent with the orthogonal position of the AHIII 12.2 TCR atop p1049/A2 and imply that AHIII 12.2 recognition of p1058/D^b assumes the canonical diagonal orientation.

There is not a set of conserved contacts that generate the common docking mode of TCR on pMHC (Baker et al., 2001; Rudolph and Wilson, 2002; Wang et al., 2002). Our data demonstrate that there is not a requirement for a conserved TCR orientation with respect to pMHC interactions or activity. However, we have identified a likely explanation for the various degrees of difference in TCR orientation atop pMHC. Two distinct populations of TCR Vα domain positions exist, and these distinct groups can be separated on the basis of CD8 dependence. The canonical group of CD8-dependent diagonal binding TCRs, 2C, A6, B7, and KB5-C20, represent one group, while a second group contains AHIII 12.2, BM3.3 and LC13, and JM22, which are all CD8 independent. Studies have shown that 2C and KB5-C20 are CD8 dependent (Daniels and Jameson, 2000; Guimezanes et al., 2001). In addition, A6 and B7 have shown dependence on CD8 in CTL assays using anti-CD8 antibodies (data not shown). Similarly, AHIII 12.2 and BM3.3 are CD8 independent with respect to their cocrystalized pMHC, as the presence of anti-CD8 blocking antibody does not alter recognition (Buslepp et al., 2003; Guimezanes et al., 2001). Vβ17 containing Flu matrix peptide (MP)-specific TCR clones, such as JM22, are remarkably conserved between different donors (Moss et al., 1995), and Vβ17 TCR are CD8 independent in studies with blocking human anti-CD8 antibody (Lawson et al., 2001). Thus, we infer that JM22 is CD8 independent. Finally, soluble CD8$\alpha\alpha$ (Sewell et al., 1999) does not inhibit lysis of EBV-infected HLA B8 positive cell lines (LCLs) by LC13 (S. Burrows, personal communication); however, a FLU-B8-reactive CTL clone, PP36, is inhibited by soluble CD8$\alpha\alpha$ in the same assay. These data suggest that the orientation of TCR on pMHC, and in particular the position of the TCR Vα domain, ensures optimal coordination of the CD8 coreceptor with the TCR/pMHC complex. Additionally, these data imply that the TCR Vα positions of AHIII 12.2, BM3.3, JM22, and LC13 sterically hinder association of the TCR/pMHC complex with CD8.

CD8 is expressed as an α/β heterodimer on the majority of $CD8^+$ α/β TCR^+ T cells. The intracellular tail of the CD8β chain is palmitylated to enhance association with cholesterol-containing microdomains (Arcaro et al., 2000). Two cysteines in the intracellular tail of CD8α share coordination of a zinc with the src-family kinase, $p56^{lck}$ (Lin et al., 1998; Shaw et al., 1990; Turner et al., 1990). The N-terminal Ig-like V domains of CD8 binds residues in the α2 and α3 domains of the class I MHC heavy chain (Gao et al., 1997; Kern et al., 1998; Sewell et al., 1999). Additionally, interactions between the CD8 stalk region and the FG loop in the constant domain of the TCR β chain have been proposed previously (Sasada et al., 2002). Upon binding of pMHC by TCR and CD8, $p56^{lck}$ is brought in proximity to the ITAMs of CD3ζ, resulting in ITAM phosphorylation and initiation of the T cell signaling cascade.

The necessity of CD8 for positive selection of Class I-restricted thymocytes has been recognized for several years. Knockout mice lacking either CD8α or CD8β have few if any $CD8^+$ T cells, indicating that double positive T cells do not transition to the CD8 single positive stage when CD8 is absent (Crooks and Littman, 1994; Fung-Leung et al., 1991, 1994). Additionally, injection of blocking anti-CD8 antibodies into sublethally irradiated mice results in a selective loss of $CD8^+$ thymocytes (Ramsdell and Fowlkes, 1989). During T cell development, double positive thymocytes undergo positive and negative selection during the transition into mature single positive T cells, and these selection processes are mediated by the affinity of MHC for TCR (Sebzda et al., 1999). Positive selection involves TCR recognition of self-peptide/self-MHC complexes, yet the affinity of the TCR/pMHC interaction during positive selection is at least an order of magnitude lower than that necessary for TCR recognition of antigenic pMHC (Alam et al., 1996). In order to reconcile this disparity, recent data suggest that CD8 contains poorly sialylated O-glycans during the developmental stage, greatly increasing its affinity for pMHC (Daniels et al., 2001; Moody et al., 2001), much more so than is predicted for CD8/pMHC interactions based upon Biacore experiments (Garcia et al., 1996b; Kern et al., 1999; Wyer et al., 1999). Thus, an increased affinity between pMHC and CD8, in spite of a decrease in affinity between TCR and pMHC, accounts for the interaction between TCR and self-pMHC during positive selection. What then is the purpose of TCR orientation?

Our work provides unique structural insights into the requirements for CD8 in T cell positive selection. Since the first structure of a TCR/pMHC complex was determined, it has been suggested that TCR orientation acts as a "filtration" step during positive selection in the thymus, "selecting" TCR that bind pMHC in a diagonal manner (Bankovich and Garcia, 2003; Garboczi et al., 1996). We propose that the interaction of self-pMHC complexes with TCR during positive selection requires a precise orientation for correct positioning of pMHC and TCR with respect to CD8. We believe that TCR recognition during development involves a type of "lock and key" mechanism for the interaction of TCR with the self-pMHC/CD8 complex that is only present during selection due to inadequately sialylated O-glycans (Daniels et al., 2001; Moody et al., 2001). This filter allows only TCR that bind in a specific orientation to "fit" with self-pMHC/CD8, and thus survive positive selection via initiation of the appropriate signaling transduction cascade (Figure 4). In the absence of the correct geometry between TCR, MHC, and CD8, no signal would be produced and positive selection would not occur. This proposed mechanism explains how TCR recognizes self-pMHC with low affinity during T cell development, yet higher affinity TCR/pMHC interactions are required for T cell activation in the periphery. While we assume selection would occur in a similar manner for $CD4^+$ T cells, we expect the structural differences between CD4 and CD8 molecules to necessitate a different TCR domain positioning. At this point there is not enough structural information on Class II MHC-restricted TCRs to ade-

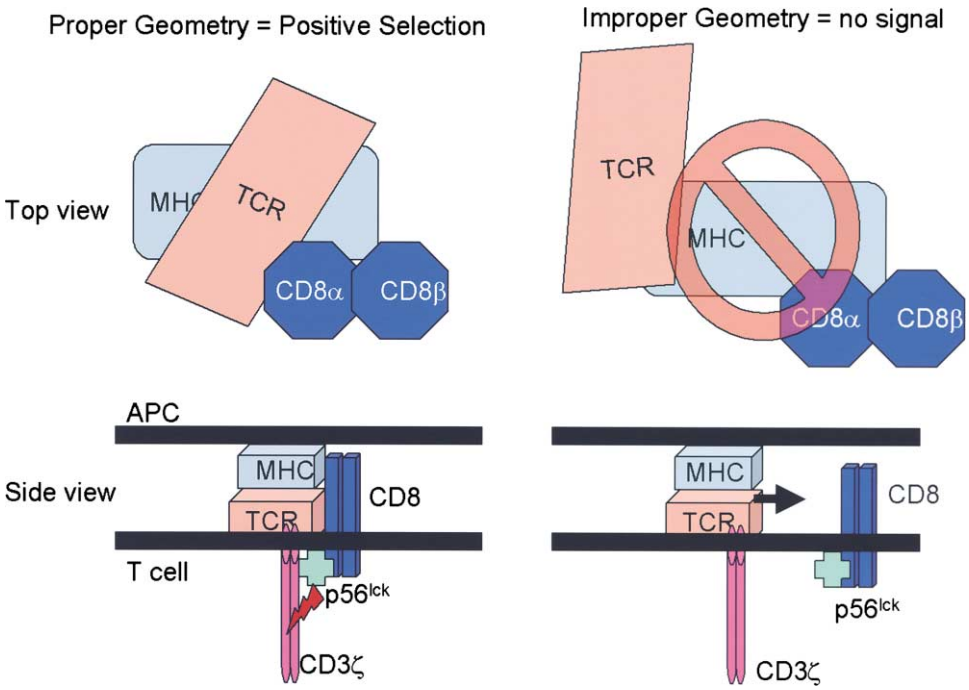

Figure 4. Model for CD8-Dependent and CD8-Independent T Cell Signaling

(Left) The TCR docks diagonally with pMHC that allows for correct positioning of CD8α/β heterodimer on the left. Positioning of CD8 juxtaposes $p56^{lck}$ with the CD3ζ chain ITAM and begins the signaling cascade.

(Right) In the CD8-independent example, the affinity of TCR for pMHC is such that CD8 is recruited to the immunological synapse in the absence of binding to MHC. The local concentration of $p56^{lck}$ is sufficient to phosphorylate CD3ζ ITAMS without direct juxtaposition. CD8 independence is unlikely to happen during T cell selection because the increased affinity would trigger negative selection.

quately predict how selection of $CD4^+$ TCR may occur. Finally, our proposed geometric filtering model for positive selection would be consistent with either instructional or stochastic lineage commitment.

Several groups have shown that increasing the affinity between TCR and pMHC will result in positive selection even in the absence of CD8 (Goldrath et al., 1997; Sherman et al., 1992). Yet these T cells positively selected due to expression of a TCR with high affinity for self-pMHC are removed during negative selection (Sebzda et al., 1999). We suggest that those TCR that are CD8 independent have increased affinity for self-pMHC, and typically are removed during negative selection. Both the AHIII 12.2 and BM3.3 TCR were selected during T cell development on a different genetic background than the pMHC in their cocrystal structures; AHIII 12.2 was selected on a mouse $H2^b$ background, while BM3.3 was selected on an $H2^k$ background. Additionally, both the AHIII 12.2 and BM3.3 TCR are of very high affinity in comparison to that of typical syngeneic TCR/pMHC interactions (Buslepp et al., 2003; Garcia et al., 1999; Reiser et al., 2000). Therefore, the Vα domain positions of AHIII 12.2 and BM3.3 atop their crossreactive ligands are a snapshot of additional Vα chain orientations found in the absence of selective pressures imposed by CD8 during thymic development. Finally, the KB5-C20 TCR is alloreactive, but adopts the canonical Vα domain position during recognition of $pKB1/K^b$. As KB5-C20 is CD8 dependent and interacts with $pKB1/K^b$ with low affinity we believe that this example only strengthens the idea that CD8 dependence is determined by Vα domain positioning. The basis for the considerable differences in functional characteristics between the KB5-C20 and BM3.3 alloreactive systems has been described previously (Guimezanes et al., 2001).

The LC13 and JM22 TCR are two examples of immunodominant TCR, and interestingly, both are CD8 independent. LC13 recognizes Epstein Barr (EBV) viral peptide FLRGRAYGL complexed with HLA-B8, while JM22 recognizes the influenza A MP in complex with HLA-A2. We predict that during selection, these two TCR interact with self-pMHC in a diagonal orientation with the Vα domain in the canonical position. Yet both the MP/A2 and FLRGRAYGL/B8 pMHC ligands provide a unique molecular surface that induces an enhanced, albeit noncanonical, fit for the JM22 and LC13 TCR, respectively (Kjer-Nielsen et al., 2003; Stewart-Jones et al., 2003), when encountered in the periphery. The enhanced fit likely permits the CD8-independence of these two TCRs, and conveys superior expansion of a clonal, immunodominant T cell population. As EBV causes persistent infection in ~90% of adults (Moss et al., 2001) and MP-specific T cells are continuously present in the memory pool, this scheme may be a tactic employed by viruses to impair the T cell immune response. Several molecular mechanisms used by viruses to evade detection by the immune system have already been characterized (Ploegh, 1998).

An AHIII 12.2 TCR transgenic mouse is being generated to explore the T cell repertoire selected when TCR/pMHC binding is non-canonical during T cell development. We expect these mice and future experiments to allow us to conclusively show that geometric filtering is a required part of positive selection.

Experimental Procedures

Protein Production and Crystallization

The α and β chains of the soluble AHIII 12.2 TCR were produced in *E. coli* as inclusion bodies and refolded to the native state in vitro as described (Buslepp et al., 2003). Similarly, Class I MHC was produced as inclusion bodies in *E. coli* and refolded (Garboczi et al., 1992). Crystals of the AHIII 12.2/p1049/A2 complex were grown by hanging drop, vapor diffusion, using a 1:1 mixture containing 10 mg/ml of each protein. Initial crystals were grown in 12% PEG 8000, 25 mM HEPES (pH 7.1), 1 M NaCl conditions and were improved by macro seeding in identical conditions except substituting with PEG 3350. Crystals were transferred to mother liquor containing 25% glycerol cryoprotectant. Crystals diffracted to 2.6 Å on a rotating anode, but were significantly improved by data collection with synchrotron radiation. Data were collected at NSLS beamline X12b at 12189ev (1.017 Å), at a distance of 150 mm using 1.0° oscillations. The refined mosaicity is 0.51°. Data were indexed and scaled with HKL2000 (Otwinowski, 1997). Data statistics are shown in Table 1.

Structure Determination and Refinement

The phases for the cocrystal were determined by molecular replacement using AMoRe as implemented in the CCP4 package (Dodson, 1997; Navaza, 1997). The search models used were p1049/A2 (1BOG) and the 2C TCR (1TCR). There was a single rotation solution. Visual inspection of the resulting packing based on the molecular replacement solution showed sufficient space for a second TCR/pMHC complex. Examination of the translation results showed a second translation solution almost half a cell length along the crystallographic a and b axes with the same rotations as the first solution. The final correlation coefficient after fitting both complexes was 57.0 and the R_{fac} was 36.4%. Temperature factors were set to 20.0 and the data were rigid body fit with Refmac 5.0 (Murshudov et al., 1997). Positional refinement using both noncrystallographic symmetry restraints and TLS refinement (Winn et al., 2001) to correct for domain-specific anisotropic temperature factors was performed iteratively with manual intervention using O (Jones et al., 1991). Peptide p1049 was not included in the model until the R_{free} dropped below 30.0% as an internal control for model bias. When the statistics did not improve over two subsequent rounds as described above and the R_{free} was below 30%, waters were added using Arp (Perrakis et al., 2001). All waters were examined visually and had to be within 2.6–3.2 Å from two hydrogen bond donor or acceptors to be included in the model. The refinement statistics for the final model are shown in Table 1.

Acknowledgments

The authors wish to thank Dr. David Margulies (NIH) and the Collins, Frelinger, and Appella labs for stimulating discussions. Additionally, we thank J. Houtman for critical reading of the manuscript. We also thank Jason Snyder, Laurie Betts, and the staff at Brookhaven National Laboratories, National Synchrotron Light Source for assistance in crystallization and data collection.

Received: May 27, 2003
Revised: August 5, 2003
Accepted: August 11, 2003
Published: October 14, 2003

References

Alam, S.M., Travers, P.J., Wung, J.L., Nasholds, W., Redpath, S., Jameson, S.C., and Gascoigne, N.R. (1996). T-cell-receptor affinity and thymocyte positive selection. Nature *381*, 616–620.

Arcaro, A., Gregoire, C., Boucheron, N., Stotz, S., Palmer, E., Malissen, B., and Luescher, I.F. (2000). Essential role of CD8 palmitoylation in CD8 coreceptor function. J. Immunol. *165*, 2068–2076.

Bachmann, M.F., Salzmann, M., Oxenius, A., and Ohashi, P.S. (1998). Formation of TCR dimers/trimers as a crucial step for T cell activation. Eur. J. Immunol. *28*, 2571–2579.

Baker, B.M., Turner, R.V., Gagnon, S.J., Wiley, D.C., and Biddison, W.E. (2001). Identification of a crucial energetic footprint on the al helix of human histocompatibility leukocyte antigen (HLA)-A2 that provides functional interactions for recognition by tax peptide/HLA-A2-specifrc T cell receptors. J. Exp. Med. *193*, 551–562.

Bankovich, A.J., and Garcia, K.C. (2003). Not just any T cell receptor will do. Immunity *18*, 7–11.

Buslepp, J., Kerry, S.E., Loftus, D., Frelinger, J.A., Appella, E., and Collins, E.J. (2003). High affinity xenoreactive TCR:MHC interaction recruits CD8 in absence of binding to MHC. J. Immunol. *170*, 373–383.

Carson, M. (1987). Ribbon models of macromolecules. J. Mol. Graph. *5*, 103–106.

Crooks, M.E., and Littman, D.R. (1994). Disruption of T lymphocyte positive and negative selection in mice lacking the CD8 beta chain. Immunity *1*, 277–285.

Daniels, M.A., Devine, L., Miller, J.D., Moser, J.M., Lukacher, A.E., Altman, J.D., Kavathas, P., Hogquist, K.A., and Jameson, S.C. (2001). CD8 binding to MHC class I molecules is influenced by T cell maturation and glycosylation. Immunity *15*, 1051–1061.

Daniels, M.A., and Jameson, S.C. (2000). Critical role for CD8 in T cell receptor binding and activation by peptide/major histocompatibility complex multimers. J. Exp. Med. *191*, 335–346.

Davis, M.M., and Bjorkman, P.J. (1988). T-cell antigen receptor genes and T-cell recognition. Nature *334*, 395–402.

Ding, Y.H., Smith, K.J., Garboczi, D.N., Utz, U., Biddison, W.E., and Wiley, D.C. (1998). Two human T cell receptors bind in a similar diagonal mode to the HLA-A2/Tax peptide complex using different TCR amino acids. Immunity *8*, 403–411.

Ding, Y.H., Baker, B.M., Garboczi, D.N., Biddison, W.E., and Wiley, D.C. (1999). Four A6-TCR/peptide/HLA-A2 structures that generate very different T cell signals are nearly identical. Immunity *11*, 45–56.

Dodson, E.J., Winn, M., and Ralph, A. (1997). Collaborative Computational Project, Number 4: Providing Programs for Protein Crystallography. In Methods Enzymol., C.W. Carter and R.M. Sweet, eds. (New York, NY, Academic Press), pp. 620–633.

Engelhard, V.H., and Benjamin, C. (1982). Isolation and characterization of monoclonal mouse cytotoxic T lymphocytes with specificity for HLA-A,B or -DR alloantigens. J. Immunol. *129*, 2621–2629.

Fung-Leung, W.P., Schilham, M.W., Rahemtulla, A., Kundig, T.M., Vollenweider, M., Potter, J., van Ewijk, W., and Mak, T.W. (1991). CD8 is needed for development of cytotoxic T cells but not helper T cells. Cell *65*, 443–449.

Fung-Leung, W.P., Kundig, T.M., Ngo, K., Panakos, J., De Sousa-Hitzler, J., Wang, E., Ohashi, P.S., Mak, T.W., and Lau, C.Y. (1994). Reduced thymic maturation but normal effector function of CD8+ T cells in CD8 beta gene-targeted mice. J. Exp. Med. *180*, 959–967.

Gao, G.F., Tormo, J., Gerth, U.C., Wyer, J.R., McMichael, A.J., Stuart, D.I., Bell, J.I., Jones, E.Y., and Jakobsen, B.K. (1997). Crystal structure of the complex between human CD8alpha(alpha) and HLA-A2. Nature *387*, 630–634.

Garboczi, D.N., and Biddison, W.E. (1999). Shapes of MHC restriction. Immunity *10*, 1–7.

Garboczi, D.N., Hung, D.T., and Wiley, D.C. (1992). HLA-A2-peptide complexes: refolding and crystallization of molecules expressed in Escherichia coli and complexed with single antigenic peptides. Proc. Natl. Acad. Sci. USA *89*, 3429–3433.

Garboczi, D.N., Ghosh, P., Utz, U., Fan, Q.R., Biddison, W.E., and Wiley, D.C. (1996). Stucture of the complex between human T-cell receptor, viral peptide and HLA-A2. Nature *384*, 134–141.

Garcia, K.C., Degano, M., Stanfield, R.L., Brunmark, A., Jackson, M.R., Peterson, P.A., Teyton, L., and Wilson, I.A. (1996a). An alpha-

beta T cell receptor structure at 2.5 A and its orientation in the TCR-MHC complex. Science *274*, 209–219.

Garcia, K.C., Scott, C.A., Brunmark, A., Carbone, F.R., Peterson, P.A., Wilson, I.A., and Teyton, L. (1996b). CD8 enhances formation of stable T-cell receptor/MHC class I molecule complexes. Nature *384*, 577–581.

Garcia, K.C., Degano, M., Pease, L.R., Huang, M., Peterson, P.A., Teyton, L., and Wilson, I.A. (1998). Structural basis of plasticity in T cell receptor recognition of a self peptide-MHC antigen. Science *279*, 1166–1172.

Garcia, K.C., Teyton, L., and Wilson, L.A. (1999). Structural basis of T cell recognition. Annu. Rev. Immunol. *17*, 369.

Germain, R.N. (2002). T-cell development and the CD4-CD8 lineage decision. Nat. Rev. Immunol. *2*, 309–322.

Goldrath, A.W., Hogquist, K.A., and Bevan, M.J. (1997). CD8 lineage commitment in the absence of CD8. Immunity *6*, 633–642.

Guimezanes, A., Barrett-Wilt, G.A., Gulden-Thompson, P., Shabanowitz, J., Engelhard, V.H., Hunt, D.F., Schmitt-Verhulst, A.M., and Engelhardt, V.H. (2001). Identification of endogenous peptides recognized by in vivo or in vitro generated alloreactive cytotoxic T lymphocytes: distinct characteristics correlated with CD8 dependence. Eur. J. Immunol. *31*, 421–432.

Henderson, R.A., Cox, A.L., Sakaguchi, K., Appella, E., Shabanowitz, J., Hunt, D.F., and Engelhard, V.H. (1993). Direct identification of an endogenous peptide recognized by multiple HLA-A2.1-specific cytotoxic T cells. Proc. Natl. Acad. Sci. USA *90*, 10275–10279.

Hennecke, J., Carfi, A., and Wiley, D.C. (2000). Structure of a covalently stabilized complex of a human alphabeta T-cell receptor, influenza HA peptide and MHC class II molecule, HLA-DR1. EMBO J. *19*, 5611–5624.

Holler, P.D., Chlewicki, L.K., and Kranz, D.M. (2003). TCRs with high affinity for foreign pMHC show self-reactivity. Nat. Immunol. *4*, 55–62.

Jones, T.A., Zou, J.-Y., Cowan, S.W., and Kjeldgaard, M. (1991). Improved methods for building protein models in electron density maps and the location of errors in these models. Acta Crystallogr. A *A47*, 110–119.

Kern, P.S., Teng, M.K., Smolyar, A., Liu, J.H., Liu, J., Hussey, R.E., Spoerl, R., Chang, H.C., Reinherz, E.L., and Wang, J.H. (1998). Structural basis of CD8 coreceptor function revealed by crystallographic analysis of a murine CD8alphaalpha ectodomain fragment in complex with H-2Kb. Immunity *9*, 519–530.

Kern, P., Hussey, R.E., Spoerl, R., Reinherz, E.L., and Chang, H.C. (1999). Expression, purification, and functional analysis of murine ectodomain fragments of CD8alphaalpha and CD8alphabeta dimers. J. Biol. Chem. *274*, 27237–27243.

Kjer-Nielsen, L., Clements, C.S., Purcell, A.W., Brooks, A.G., Whisstock, J.C., Burrows, S.R., McCluskey, J., and Rossjohn, J. (2003). A structural basis for the selection of dominant alphabeta T cell receptors in antiviral immunity. Immunity *18*, 53–64.

Lawrence, M.C., and Coleman, P.M. (1993). Shape complementarity at protein/protein interfaces. J. Mol. Biol. *234*, 946–950.

Lawson, T.M., Man, S., Wang, E.C., Williams, S., Amos, N., Gillespie, G.M., Moss, P.A., and Borysiewicz, L.K. (2001). Functional differences between influenza A-specific cytotoxic T lymphocyte clones expressing dominant and subdominant TCR. Int. Immunol. *13*, 1383–1390.

Lin, R.S., Rodriguez, C., Veillette, A., and Lodish, H.F. (1998). Zinc is essential for binding of p56(lck) to CD4 and CD8alpha. J. Biol. Chem. *273*, 32878–32882.

Loftus, D.J., Chen, Y., Covell, D.G., Engelhard, V.H., and Appella, E. (1997). Differential contact of disparate class I/peptide complexes as the basis for epitope cross-recognition by a single T cell receptor. J. Immunol. *158*, 3651–3658.

Manning, T.C., Schlueter, C.J., Brodnicki, T.C., Parke, E.A., Speir, J.A., Garcia, K.C., Teyton, L., Wilson, I.A., and Kranz, D.M. (1998). Alanine scanning mutagenesis of an alphabeta T cell receptor: mapping the energy of antigen recognition. Immunity *8*, 413–425.

Mason, D. (1998). A very high level of crossreactivity is an essential feature of the T-cell receptor. Immunol. Today *19*, 395–404.

Moody, A.M., Chui, D., Reche, P.A., Priatel, J.J., Marth, J.D., and Reinherz, E.L. (2001). Developmentally regulated glycosylation of the CD8alphabeta coreceptor stalk modulates ligand binding. Cell *107*, 501–512.

Moss, P.A., Rowland-Jones, S.L., Frodsham, P.M., McAdam, S., Giangrande, P., McMichael, A.J., and Bell, J.I. (1995). Persistent high frequency of human immunodeficiency virus-specific cytotoxic T cells in peripheral blood of infected donors. Proc. Natl. Acad. Sci. USA *92*, 5773–5777.

Moss, D.J., Burrows, S.R., Silins, S.L., Misko, I., and Khanna, R. (2001). The immunology of Epstein-Barr virus infection. Philos. Trans. R. Soc. Lond. B Biol. Sci. *356*, 475–488.

Murshudov, G.N., Vagin, A.A., and Dodson, E.J. (1997). Refinement of molecular structures by maximum-likelihood method. Acta Crystallogr. D *53*, 240–255.

Navaza, J.S.P. (1997). AMoRe: an automated molecular replacement program package. In Methods Enzymol., C.W. Carter and R.M. Sweet, eds. (New York: Academic Press), pp. 581–594.

Nicholls, A., Sharp, K.A., and Honig, B. (1991). Protein folding and association: insights from the interfacial and thermodynamic properties of hydrocarbons. Proteins *11*, 281–296.

Otwinowski, Z.M. W. (1997). Processing of X-ray diffraction data collected in oscillation mode. In Methods Enzymol., C.W.J.S. Carter, ed. (New York: Academic Press), pp. 307–326.

Pannu, N.S., and Reed, R.J. (1996). Improved structure refinement through maximum likelihood. Acta Cryst. A *52*, 659–668.

Perrakis, A., Harkiolaki, M., Wilson, K.S., and Lamzin, V.S. (2001). ARP/wARP and molecular replacement. Acta Crystallogr. D Biol. Crystallogr. *57*, 1445–1450.

Ploegh, H.L. (1998). Viral strategies of immune evasion. Science *280*, 248–253.

Ramsdell, F., and Fowlkes, B.J. (1989). Engagement of CD4 and CD8 accessory molecules is required for T cell maturation. J. Immunol. *143*, 1467–1471.

Reinherz, E.L., Tan, K., Tang, L., Kern, P., Liu, J., Xiong, Y., Hussey, R.E., Smolyar, A., Hare, B., Zhang, R., et al. (1999). The crystal structure of a T cell receptor in complex with peptide and MHC class II. Science *286*, 1913–1921.

Reiser, J.B., Darnault, C., Guimezanes, A., Gregoire, C., Mosser, T., Schmitt-Verhulst, A.M., Fontecilla-Camps, J.C., Malissen, B., Housset, D., and Mazza, G. (2000). Crystal structure of a T cell receptor bound to an allogeneic MHC molecule. Nat. Immunol. *1*, 291–297.

Reiser, J.B., Gregoire, C., Darnault, C., Mosser, T., Guimezanes, A., Schmitt-Verhulst, A.M., Fontecilla-Camps, J.C., Mazza, G., Malissen, B., and Housset, D. (2002). A T cell receptor CDR3beta loop undergoes conformational changes of unprecedented magnitude upon binding to a peptide/MHC class I complex. Immunity *16*, 345–354.

Reiser, J.B., Darnault, C., Gregoire, C., Mosser, T., Mazza, G., Kearney, A., van der Merwe, P.A., Fontecilla-Camps, J.C., Housset, D., and Malissen, B. (2003). CDR3 loop flexibility contributes to the degeneracy of TCR recognition. Nat. Immunol. *4*, 241–247.

Rotzschke, O., Falk, K., and Strominger, J.L. (1997). Superactivation of an immune response triggered by oligomerized T cell epitopes. Proc. Natl. Acad. Sci. USA *94*, 14642–14647.

Rudolph, M.G., and Wilson, I.A. (2002). The specificity of TCR/pMHC interaction. Curr. Opin. Immunol. *14*, 52–65.

Sasada, T., Touma, M., Chang, H.C., Clayton, L.K., Wang, J.H., and Reinherz, E.L. (2002). Involvement of the TCR Cbeta FG loop in thymic selection and T cell function. J. Exp. Med. *195*, 1419–1431.

Sebzda, E., Mariathasan, S., Ohteki, T., Jones, R., Bachmann, M.F., and Ohashi, P.S. (1999). Selection of the T cell repertoire. Annu. Rev. Immunol. *17*, 829–874.

Sewell, A.K., Gerth, U.C., Price, D.A., Purbhoo, M.A., Boulter, J.M., Gag, G.F., Bell, J.I., Phillips, R.E., and Jakobsen, B.K. (1999). Antagonism of cytotoxic T-lymphocyte activation by soluble CD8. Nat. Med. *5*, 399–404.

Shaw, A.S., Chalupny, J., Whitney, J.A., Hammond, C., Amrein, K.E., Kavathas, P., Sefton, B.M., and Rose, J.K. (1990). Short related sequences in the cytoplasmic domains of CD4 and CD8 mediate binding to the amino-terminal domain of the p56lck tyrosine protein kinase. Mol. Cell. Biol. *10*, 1853–1862.

Sherman, L.A., Hesse, S.V., Irwin, M.J., La Face, D., and Peterson, P. (1992). Selecting T cell receptors with high affinity for self-MHC by decreasing the contribution of CD8. Science *258*, 815–818.

Stewart-Jones, G.B., McMichael, A.J., Bell, J.I., Stuart, D.I., and Jones, E.Y. (2003). A structural basis for immunodominant human T cell receptor recognition. Nat. Immunol. *4*, 657–663.

Turner, J.M., Brodsky, M.H., Irving, B.A., Levin, S.D., Perlmutter, R.M., and Littman, D.R. (1990). Interaction of the unique N-terminal region of tyrosine kinase p56lck with cytoplasmic domains of CD4 and CD8 is mediated by cysteine motifs. Cell *60*, 755–765.

Wang, Z., Turner, R., Baker, B.M., and Biddison, W.E. (2002). MHC allele-specific molecular features determine peptide/HLA-A2 conformations that are recognized by HLA-A2-restricted T cell receptors. J. Immunol. *169*, 3146–3154.

Winn, M.D., Isupov, M.N., and Murshudov, G.N. (2001). Use of TLS parameters to model anisotropic displacements in macromolecular refinement. Acta Crystallogr. D *57*, 122–133.

Wyer, J.R., Willcox, B.E., Gao, G.F., Gerth, U.C., Davis, S.J., Bell, J.I., van der Merwe, P.A., and Jakobsen, B.K. (1999). T cell receptor and coreceptor CD8 alpha alpha bind peptide-MHC independently and with distinct kinetics. Immunity *10*, 219–225.

Zhao, R., Loftus, D.J., Appella, E., and Collins, E.J. (1999). Structural evidence of T cell xeno-reactivity in the absence of molecular mimicry. J. Exp. Med. *189*, 359–370.